Princeton Plasma Physics Laboratory

PPPL- 4642

PPPL- 4642

Experimental Verificatio of the Kruskal-Shafranov Stability Limit in Line-Tied Partial Toroidal Plasmas

E. Oz, C.E. Myers, M. Yamada, H. Ji, R.M.. Kulsrud and J. Xie

July, 2011

PPPL
PRINCETON PLASMA
PHYSICS LABORATORY

Prepared for the U.S. Department of Energy under Contract DE-AC02-09CH11466.

Princeton Plasma Physics Laboratory
Report Disclaimers

Full Legal Disclaimer

Trademark Disclaimer

PPPL Report Availability

Princeton Plasma Physics Laboratory:

http://www.pppl.gov/techreports.cfm

Office of Scientific and Technical Information (OSTI):

http://www.osti.gov/bridge

Related Links:

U.S. Department of Energy

Office of Scientific and Technical Information

Fusion Links

Experimental Verification of the Kruskal-Shafranov Stability Limit in Line-Tied Partial Toroidal Plasmas

E. Oz,[a] C. E. Myers, M. Yamada,[b] H. Ji, R. M. Kulsrud, and J. Xie[c]
Princeton Plasma Physics Laboratory, Princeton, NJ 08543

(Dated: 17 June 2011)

The stability properties of partial toroidal flux ropes are studied in detail in the laboratory, motivated by ubiquitous arched magnetic structures found on the solar surface. The flux ropes studied here are magnetized arc discharges formed between two electrodes in the Magnetic Reconnection Experiment (MRX) [Yamada et al., Phys. Plasmas, **4**, 1936 (1997)]. The three dimensional evolution of these flux ropes is monitored by a fast visible light framing camera, while their magnetic structure is measured by a variety of internal magnetic probes. The flux ropes are consistently observed to undergo large-scale oscillations as a result of an external kink instability. Using detailed scans of the plasma current, the guide field strength, and the length of the flux rope, we show that the threshold for kink stability is governed by the Kruskal-Shafranov limit for a flux rope that is held fixed at both ends (i.e., $q_a = 1$).

I. INTRODUCTION

Coronal loops and arcades are partial toroidal magnetic structures found on the solar surface. These arched structures intersect the dense photosphere at footpoints that are believed to be anchored or "line-tied" in place.[1] Energetic events such as coronal mass ejections (CMEs)[2] are often regarded as a consequence of instability and/or loss of equilibrium in one of these partial toroidal structures.[1,3–7] One potential CME trigger mechanism is the ideal external kink instability (see, e.g., Török and Kliem[8]). Despite rapid progress in observational capabilities, the lack of detailed magnetic measurements in crucial areas of the corona has prevented the conclusive study of kink stability in coronal magnetic structures. In contrast to remote-sensing observations, laboratory experiments offer *in situ* measurements that can contribute to the understanding of solar-relevant plasma phenomena such as kink stability.

The kink stability of a cylindrical magnetic flux rope is often quantified in terms of the so-called "safety-factor," q, which is given by

$$q(r) = \frac{2\pi}{L}\frac{rB_T}{B_P(r)}, \tag{1}$$

where r is the radial distance from the flux rope axis, B_T is the externally-applied "toroidal" magnetic field, B_P is the plasma-produced "poloidal" magnetic field, and L is the length of the flux rope. The safety factor measures the pitch of the field lines as they helically wind around the axis of the flux rope. If the field line pitch becomes too steep (i.e., q becomes too low), the flux rope will kink in response to long-wavelength magnetic perturbations. The onset of the most dangerous kink mode, the external kink, depends only on the value of the "edge" safety factor

$$q_a \equiv q(a) = \frac{(2\pi a)^2 B_T}{\mu_0 I_p L}, \tag{2}$$

where a is the minor radius of the flux rope and I_p is the total plasma current. As first derived by Kruskal and Shafranov, a flux rope will become unstable to the external kink mode when q_a drops below the $q_a = 1$ threshold.[9,10] This so-called Kruskal-Shafranov (KS) limit, which was derived assuming periodic flux rope boundary conditions, has been quite successful in explaining the stability of periodic (toroidal) laboratory plasmas such as tokamaks.[11] The analysis becomes more complicated, however, when considering bounded, non-periodic flux ropes such as those found in the solar corona.

Non-periodic flux ropes can be produced in the laboratory using magnetized discharges formed between two electrodes. The stability characteristics of such plasmas are predicted to be inherently dependent on the boundary conditions at the two flux rope footpoints. A given footpoint can either be "fixed" (where displacements vanish) or "free" (where stresses vanish). In the case where both footpoints are fixed, the flux rope is predicted to obey the standard $q_a = 1$ KS limit.[12,13] If, on the other hand, only one end of the flux rope is fixed and the other is free, the stability limit is predicted to change to $q_a = 2$.[14]

The two flux rope boundary configurations introduced above (dual-fixed and fixed/free) are of keen experimental interest. At the cathode end of the discharge, the magnetic field lines are frozen into both the conducting cathode material and the nearby plasma. This so-called "line-tying" effect ensures that at least the cathode end of the flux rope is a fixed boundary. The boundary condition at the anode end, however, is much more complicated. In fact, anode boundary conditions ranging from nearly fixed to completely free have been observed experimentally. Due to the complexity of the an-

[a] Present address: TeleSecurity Sciences, Inc., 7391 Prairie Falcon Road, Suite 150-B, Las Vegas, NV 89128, USA.
[b] Electronic mail: myamada@pppl.gov
[c] Present address: CAS Key Laboratory of Plasma Physics, Department of Modern Physics, University of Science and Technology of China, Hefei 230026, China.

ode boundary, a definitive experimental study of kink stability in solar-relevant dual-fixed-boundary flux ropes has remained elusive.

Experiments conducted in a linear device have demonstrated a variety of anode boundary conditions. First, a free boundary condition was observed in discharges where a thin flux rope is terminated by a large anode plate.[15] In these experiments, the criterion for the onset of the external kink mode was found to be $q_a = 2$, indicating that the flux rope was exhibiting fixed/free stability behavior. It is believed that a resistive sheath forms at the anode end of the flux rope that magnetically detaches it from the electrode surface. The flux rope is then able slide freely over the surface of the large anode plate. In an attempt to force the anode to instead act as a fixed boundary, several different conical electrodes were used to inhibit the movement of the flux rope's free end.[16] Six anodes with increasingly restrictive conical shapes were shown to confine the motion of the flux rope and increase its stability against the kink mode. While stability thresholds in the range of $2 \geq q_a \gtrsim 1.2$ were observed using this technique, full $q_a = 1$ fixed-boundary behavior was not achieved.

Experiments with open-ended plasma plumes have correlated the $q_a = 1$ KS limit to the onset of kink stability.[17,18] In these devices, the plasma does not interact directly with the anode; instead, it terminates at a plasma/vacuum interface as it streams away from the cathode. Though the line-tied (fixed) condition at the cathode is expected, it is not obvious that the plasma/vacuum interface should act as a second fixed boundary. Both experimental groups cite the Alfvénic discontinuity that results from a strong density gradient at the plasma/vacuum interface as a possible cause of the observed stability behavior. Because of the uncertainty surrounding this boundary condition at the open end, however, these experiments do not constitute a definitive study of kink stability in dual-fixed-boundary systems.

A third experimental study was carried out with a linear screw pinch plasma where clear evidence of a kink mode was observed.[19] Here, the mode onset is attributed to q dropping below unity in the interior of the plasma. Consequently, the authors conclude that the plasma exhibits dual-fixed-boundary stability behavior. It is interesting to note, however, that the edge q value crosses the $q_a = 2$ threshold at nearly the same time that q drops below unity inside the plasma. It is therefore conceivable that the discharge instead has a fixed/free boundary configuration. In this scenario, the external kink would trigger from $q_a = 2$ at the edge rather than from $q < 1$ internally. Thus, despite the existing body of work summarized here, we conclude that the predicted $q_a = 1$ threshold for dual-fixed-boundary kink stability has not been conclusively demonstrated in the laboratory.

In this paper, we present definitive evidence that magnetic flux ropes formed between two equally-sized electrodes do, in fact, exhibit the $q_a = 1$ KS threshold for dual-fixed-boundary stability. We quantitatively support this conclusion with stability measurements from detailed scans of the plasma current, toroidal field strength, and flux rope length. The restricted motion of the flux rope at the anode footpoint, which is required in order to have a second fixed boundary, is attributed to the direct matching between the minor radius of the anode plate and the minor radius of the flux rope (as set by the cathode). Additionally, the flux ropes studied here have a partial toroidal geometry and are therefore highly relevant to structures found in the solar corona. Several experimental groups have previously studied partial toroidal plasmas in the laboratory[20–22], but the stability properties of these plasmas were not quantitatively investigated.

II. EXPERIMENTAL SETUP

The experiments reported here were conducted in the Magnetic Reconnection Experiment (MRX) facility[23]. In order to form a partial toroidal flux rope, an arc discharge is created between two copper electrodes of equal size that are separated by a variable toroidal angle (see Fig. 1). The electrodes are copper disks of minor radius $a = 7.3$ cm. Their major radius R can be varied from 20 to 30 cm, and the angle between the electrodes Θ can be varied from 90° to 270° (Fig. 2b). The stainless steel wall of the vacuum vessel is located far away from the discharge at $R = 73.6$ cm. The electrodes are powered by a capacitor bank with typical voltages of 3–10 kV and up to 50 kJ of stored energy. The electrode circuit is constructed with a double feed-through in order to minimize its inductance. Large circular coils outside the ends of the vacuum vessel provide a z-directed strapping (equilibrium) field, B_E, of up to 200 G that is largely uniform in time and space. A separate set of eight three-turn coils thread the center of the device and produce a toroidal (θ-directed) guide field, B_T. This coil set, which is powered by a standalone 0.5 F, 450 V capacitor bank, provides up to 1500 G of toroidal field at the center of the copper electrodes.

The working gas is puffed in before the plasma is formed and fills the vacuum vessel to a uniform pressure of several mTorr. The gas puff is controlled by several piezoelectric valves that inject gas at the machine wall or through small holes in the electrodes. This configuration permits the use of a mixture of gases to achieve ionization at lower applied voltages. Experiments conducted with various gas species such as H, D, He, Ar and pressure scans from 1–100 mTorr showed few discernable changes in the flux rope dynamics. All of the experimental data that is shown in Secs. III and IV is taken from hydrogen shots where the gas was injected only at the machine wall. The fill pressures for these discharges ranged from 10–20 mTorr.

A typical flux rope discharge in MRX lasts ∼700 μs. This is substantially longer than both the Alfvén transit time ($t_A \sim 1.0$ μs) and the duration of other partial toroidal flux rope experiments, which persist for only a few microseconds.[20,21] A sample flux rope plasma cur-

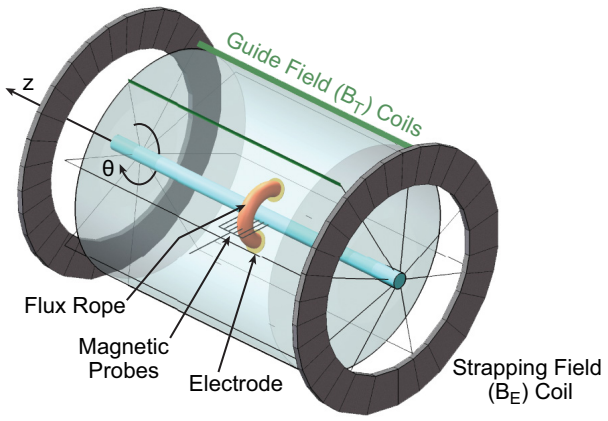

FIG. 1. A schematic of the experimental setup. A plasma arc with a major radius of 20–30 cm (orange) is maintained between two electrodes. Current through the center column (center blue and return paths green) provides the toroidal guide field, B_T, along the plasma arc; a pair of external coils (big gray circles) provides the equilibrium field (B_E) along the z direction. The plasma current provides the poloidal field that twists the field lines in the flux rope. Also shown is the 2-D magnetic probe array.

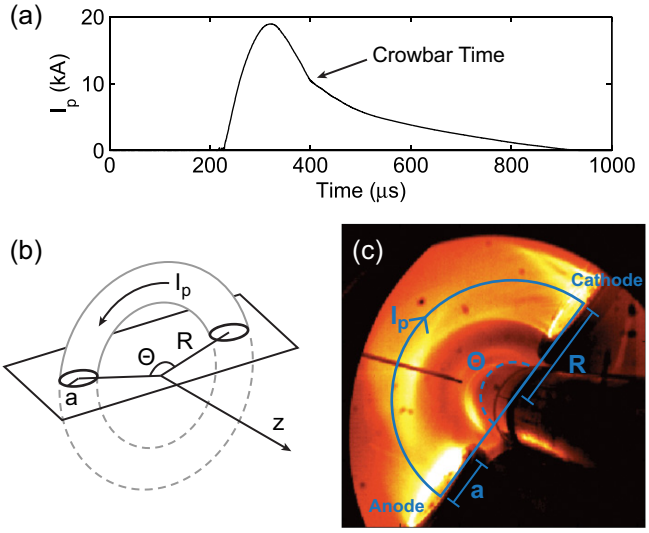

FIG. 2. (a) A typical plasma current waveform $I_p(t)$. (b) A schematic of the current loop with minor radius a and major radius R. The angle between the electrodes is designated as Θ. (c) A visible light image of a flux rope plasma taken by a fast framing camera with a 1 μs exposure time.

rent waveform $I_p(t)$ is shown in Fig. 2a. The shape of this waveform is determined by the characteristics of the driving circuit, which includes the capacitor bank, its connections to the electrodes, and the plasma arc itself. High power diodes are included in the forward part of the driving circuit such that when the "crowbar" circuit is closed at $t \simeq 400$ μs, the plasma current waveform decays monotonically thereafter as a simple L-R circuit. This monotonic decay is crucial for clearly identifying the kink stability threshold. An oscillating waveform, on the other hand, would drive the flux rope back and forth across the stability threshold, thereby significantly complicating the stability analysis.

The MRX flux rope plasmas are monitored with a variety of magnetic probes, including a rake-shaped 90 channel probe array that measures all three components of the magnetic field at 30 locations in a 2D (z-r) plane. These measurements permit the reconstruction of the current density profile within the flux rope at one toroidal location. Several additional magnetic probes are included at various other toroidal locations along the flux rope. These additional probes are 1D (radial) probes that measure the axial field profile $B_z(r)$ along their length. The radial location where each $B_z(r)$ profile reverses sign corresponds to the location of the magnetic axis of the flux rope at that toroidal location. By combining these measurements, the r-θ profile of the flux rope can be reconstructed as a function of time. This profile provides a measurement of the length of the flux rope $L(t)$ that is used in the stability analysis. The signals from each of these magnetic probes are digitized at 2.5 MHz (every 0.4 μs), which is slightly faster than the Alfvén transit time ($t_A \sim 1.0$ μs). Additionally, a fast CCD camera is used for monitoring the 3D dynamic evolution of each discharge in the visible spectrum. Frames can be captured every 4–12 μs with a 1 μs exposure time.

III. FEATURES OF THE FLUX ROPE PLASMAS

The partial toroidal flux ropes produced in MRX expand radially as a result of "hoop" forces from the arched plasma current channel. This expansion is countered by the inward force from the strapping field B_E and by tension in the entrained toroidal field B_T. Thus, because the flux ropes are driven on timescales that are much longer than the Alfvén time, they evolve through a series of equilibria where the various radial forces are in balance. Such force balance does not, however, guarantee stability. Depending on the conditions, the flux ropes are observed to undergo kink oscillations about the aforementioned partial toroidal equilibrium.

Figure 3 shows measurements from two typical discharges with different stability properties. The upper row of panels for each shot shows visible light snapshots taken at four different times by the fast framing camera (false color is added later). The lower row of panels shows the measured poloidal magnetic field vectors and the corresponding current density as measured by the rake-shaped 90 channel magnetic probe. When a substantial toroidal field is applied, the flux rope remains stable and does not move around (as in the first discharge shown in Fig. 3). However, if the toroidal field strength is lower, then the flux rope kinks wildly (as in the second discharge shown in Fig. 3). Note that the visible light amplitude correlates well with the current density. The first visi-

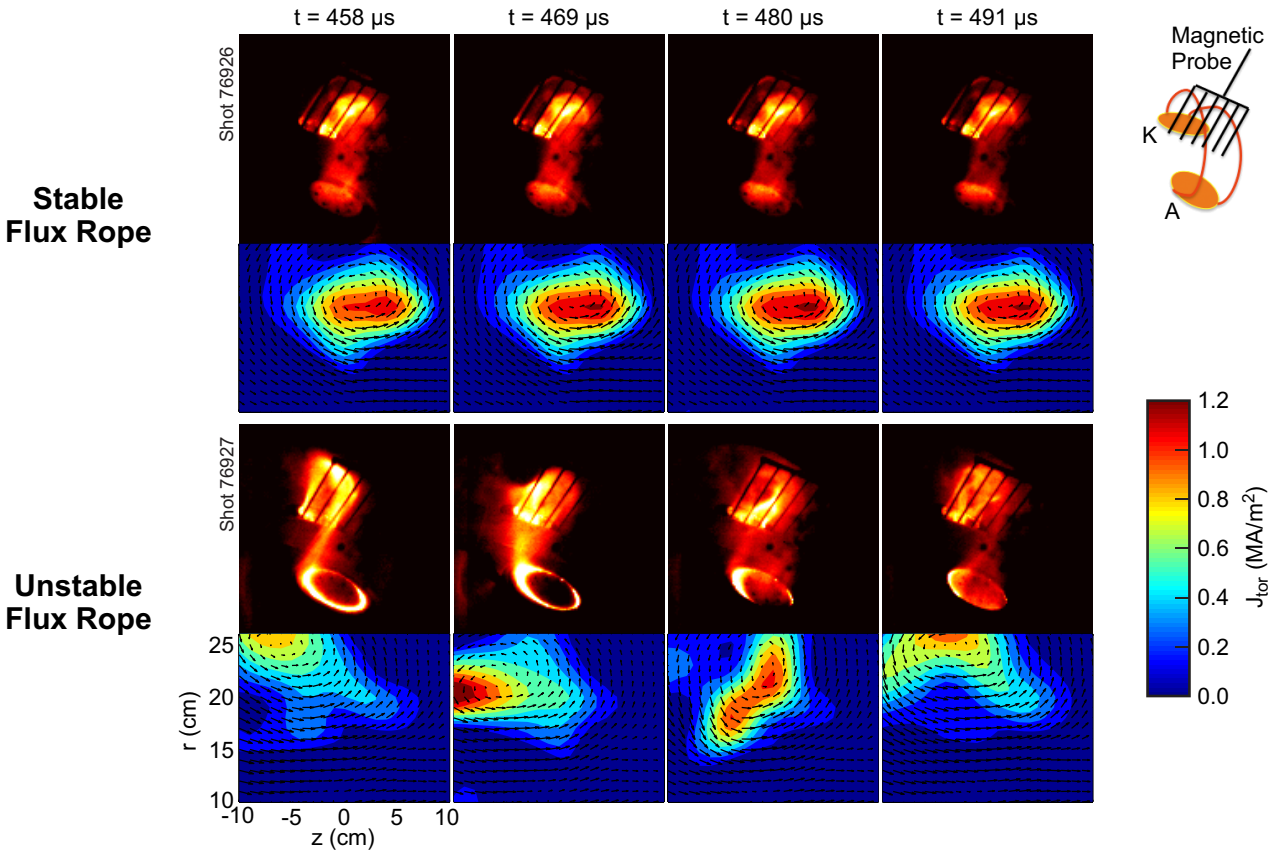

FIG. 3. Measurements from two flux ropes with different applied toroidal fields. For each flux rope, false color visible light images and magnetic measurements are shown for four different times. The diagram at the top right illustrates the electrode setup as seen by the fast framing camera. The corresponding contour plots show the measured poloidal magnetic field vectors and the resulting toroidal current density J_{tor}. The stable flux rope (top) has sufficient toroidal field to avoid kinking, while the unstable flux rope (bottom) has lower toroidal field and kinks throughout the progression.

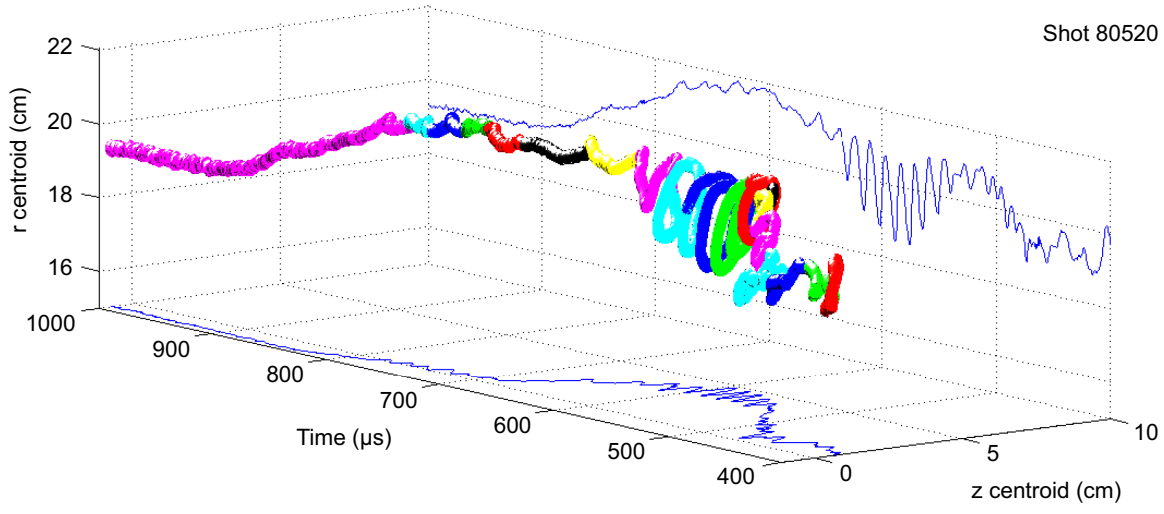

FIG. 4. Time evolution of the current density centroid (as measured by the 90 channel magnetic probe) for a plasma discharge with $\Theta = 90°$. Color is added to better visualize the motion. The two projections show the z and r position of the centroid as a function time. The flux rope is unstable early in the discharge and stable at later times when the plasma current is lower.

ble light image in the unstable case reveals some of the helical structure of the kink instability as it can be seen twisting from the cathode to the anode.

Fast framing camera movies that track the complete evolution of the flux rope show that kink unstable flux ropes in MRX make rigid body rotations. An example of these rotations can be seen in Fig. 4, which shows the time evolution of the centroid of the flux rope current density as measured by the rake-shaped 2D magnetic probe. Color is added for better visualization. The rigid body rotation of the plasma column and its eventual stabilization is clearly evident. The rotations, which are most likely driven by flows in the plasma, vary in frequency between 30–90 kHz.

IV. FLUX ROPE STABILITY CHARACTERISTICS

In order to analyze the stability properties of these flux ropes more quantitatively, we examine magnetic fluctuations that are measured by the rake-shaped 90 channel magnetic probe. In particular, we choose signals from individual magnetic pickup coils that are located near the edge of the probe. These edge coils remain outside of the flux rope for the duration of the discharge and therefore measure only external magnetic fluctuations. A sample fluctuating signal of poloidal magnetic field (δB_p) is plotted in black in each panel of Fig. 5. It is clear from these signals that the external magnetic fluctuations persist until a certain stabilization threshold is crossed where the plasma quickly ceases its kinking motion.

To identify this stabilization threshold, we focus on the transition from unstable to stable behavior that occurs between 400 and 600 μs. During this time, the flux rope equilibrium evolves rather slowly such that the stabilization time can be accurately determined. The stabilization time is measured by identifying the time where the kink oscillation amplitude drops below a few gauss without reappearing. This stabilization time will correspond to a single "threshold q_a" value (i.e., the q_a value that leads to stability), which can be determined from experimentally-measured discharge parameters. In order to calculate the threshold q_a value, the various quantities in Eq. 2 must be collected for a given discharge. Here, we assume that the flux rope minor radius a is set by the cathode minor radius and that the toroidal field B_T is given by the guide field strength at the center of the electrodes. The plasma current waveform $I_p(t)$ is measured using a current transformer and the flux rope length waveform $L(t)$ is measured by the various toroidally-distributed magnetic probes (as described in Section II). The calculated q_a evolution is plotted in blue in Fig. 5 for the four sample discharges, which each have a different electrode separation angle Θ. The angle Θ is scanned in order to modify the flux rope length because $L \gtrsim \Theta$. Because of the different flux rope lengths, the plasma stabilizes at a different time in each case. Note, however, that this time is always near $q_a \simeq 1$. In many cases, the stabilization time can also be verified by ob-

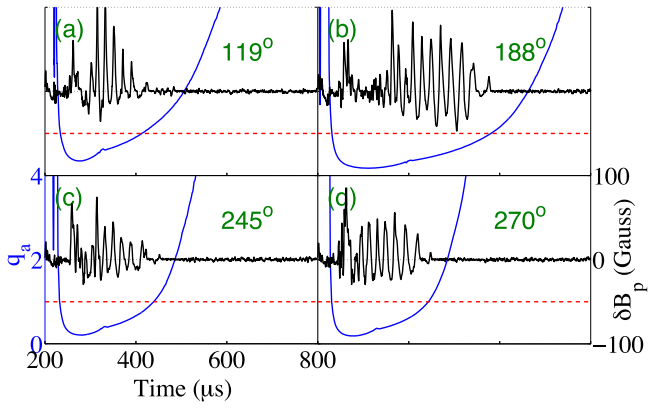

FIG. 5. Time evolution of the q_a value (blue, left axis) and magnetic fluctuation amplitude (black, right axis) for several flux ropes of varying electrode separation angle with $a = 7.3$ cm and $R \simeq 19.5$ cm. The KS stability threshold ($q_a = 1$) is drawn in red. The fluctuation traces are taken from one of the pickup coils in the 2D 90 channel probe array that is near the edge of the plasma. The fluctuations that result from the external kinking and rotation of the plasma column stop when $q_a \simeq 1$.

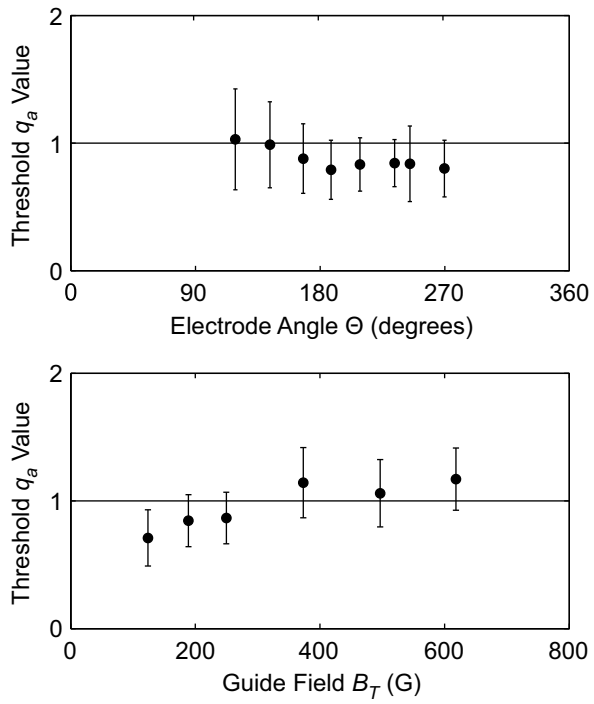

FIG. 6. (a) The measured threshold q_a value as a function of electrode separation angle. Here $B_T = 120$ G and $a = 7.3$ cm. The black solid line marks the $q_a = 1$ Kruskal-Shafranov limit. (b) The measured threshold q_a value as a function of guide field strengh B_T. Here the electrode angle is $\Theta = 270°$ and again $a = 7.3$ cm. The error bars are calculated by combining the uncertainty in the individual threshold q_a measurements with the statistical variation over multiple shots.

serving changes in the fast camera images.

We can now rigorously test the applicability of the Kruskal-Shafranov limit introduced earlier in this paper to the partial toroidal flux ropes produced in MRX. This is done by independently scanning the various quantities that modify the edge safety factor q_a. Since the plasma current I_p is already scanned within each discharge by the rise and fall of the current waveform, we focus here on scans of the electrode separation angle Θ (which changes the flux rope length L) and of the toroidal (guide) field B_T. The collection of threshold q_a values obtained from these parameter scans is shown in the two panels of Fig. 6. It is clear that in both cases the stabilization threshold remains close to $q_a = 1$ throughout the scans. This serves to verify that the KS theory captures the key physics of stability in these partial toroidal flux ropes.

As mentioned in the introduction, if the flux rope were instead free to move at one end, then the stabilization threshold is predicted to change to $q_a = 2$. This behavior is clearly not observed here. It is also worth noting that if both ends of the flux rope were free to move, the stabilization threshold would also be $q_a = 1$. We are able to rule out this possibility, however, by examining the envelope of the kink oscillations in these flux ropes. The toroidally-distributed array of 1D magnetic probes measures the displacement of the flux rope as a result of its kinking motion. We observe that the displacement amplitude is at its largest near the midpoint between the electrodes and at its smallest at the electrodes, especially the cathode. Thus we conclude that these partial toroidal plasmas obey the $q_a = 1$ Kruskal-Shafranov limit for non-periodic flux ropes with two fixed boundaries.

V. SUMMARY AND DISCUSSION

In summary, the stability characteristics of line-tied partial toroidal flux ropes formed between two electrodes of the same size have been examined in the laboratory. Magnetics measurements clearly show that the external kink stability threshold for these plasmas is governed by the Kruskal-Shafranov limit for a flux rope with two fixed boundaries ($q_a = 1$). This behavior was verified across a wide range of discharge parameters using scans of the applied toroidal field, the plasma length, and the plasma current. Despite several preexisting experimental studies of flux rope stability, this work represents the first definitive identification of $q_a = 1$ stability in laboratory flux ropes with two fixed boundaries.

As outlined in the introduction, the difficulty in experimentally identifying $q_a = 1$ stability behavior is largely due to the uncertainty and variability of the boundary condition at the anode. This can result, for example, from the formation of a resistive sheath near the anode surface or from the presence of a plasma/vacuum interface at the anode end of the discharge. In the experiments presented here, we believe that the fixed-boundary behavior at the anode is a result of the direct matching of the anode minor radius to the minor radius of the flux rope, which is set by the cathode size. Thus, even if a resistive sheath forms as described in Refs. 14–16, the limited extent of the anode surface inhibits the motion of the end of the flux rope such that the anode appears as a second fixed boundary to the flux rope plasma. This direct matching condition does not exist in any of the prior linear flux rope experiments.[15–19]

The results present here also represent the first experimental identification of $q_a = 1$ stability in a partial toroidal system. Though this lack of dependence on toroidicity is not particularly surprising given the success of the KS theory in explaining tokamak stability, it does reinforce the applicability of these results to the kink stability properties of other partial toroidal plasmas such as those found in the solar corona.

There are several important extensions of these partial toroidal flux rope experiments that will be investigated in the near future. These include studying cases where the anode is much larger than the cathode in order to permit the plasma column to move freely at one end. As mentioned, the stability criteria is predicted to change to $q_a = 2$ for this case. Another area of interest concerns the evolution and force balance of the equilibria observed in these experiments. The equilibrium reconstruction measurements used in this paper for stability analysis are being further developed for use in comprehensive studies of these partial toroidal equilibria.

ACKNOWLEDGMENTS

The authors would like to thank R. Cutler for technical contributions. This manuscript has been authored by Princeton University and collaborators under Contract Number DE-AC02-09CH11466 with the U.S. Department of Energy. The publisher, by accepting this article for publication, acknowledges that the United States Government retains a non-exclusive, paid-up, irrevocable, world-wide license to publish or reproduce the published form of this manuscript, or allow others to do so, for United States Government purposes.

[1] J. Chen, Astrophys. J., **338**, 453 (1989).
[2] N. Crooker, J. A. Joselyn, and J. Feynman, eds., *Coronal Mass Ejections* (American Geophysical Union Monograph 99, 1997).
[3] T. G. Forbes, J. Geophys. Res., **95**, 11919 (1990).
[4] Z. Mikić and J. A. Linker, Astrophys. J., **430**, 898 (1994).
[5] B. C. Low, Solar Phys., **167**, 217 (1996).
[6] S. K. Antiochos, C. R. DeVore, and J. A. Klimchuk, Astrophys. J., **510**, 485 (1999).
[7] P. A. Isenberg and T. G. Forbes, The Astrophysical Journal, **670**, 1453 (2007).
[8] T. Török and B. Kliem, Astrophys. J., **630**, L97 (2005).
[9] M. Kruskal and J. L. Tuck, Royal Society of London Proceedings Series A, **245**, 222 (1958).
[10] V. Shafranov, At. Energy, **5**, 38 (1956).
[11] J. Wesson, *Tokamaks* (Clarendon Press, Oxford, 1987).
[12] I. M. Lanskii and A. I. Shchetnikov, Sov. J. Plasma Phys., **16**, 322 (1990).
[13] C. C. Hegna, Phys. Plasmas, **11**, 4230 (2004).

[14]D. D. Ryutov, I. Furno, T. P. Intrator, S. Abbate, and T. Madziwa-Nussinov, Phys. Plasmas, **13**, 2105 (2006).
[15]I. Furno, T. P. Intrator, D. D. Ryutov, S. Abbate, *et al.*, Phys. Rev. Lett., **97**, 015002 (2006).
[16]X. Sun, T. P. Intrator, L. Dorf, I. Furno, and G. Lapenta, Phys. Rev. Lett., **100**, 205004 (2008).
[17]S. C. Hsu and P. M. Bellan, Phys. Rev. Lett., **90**, 215002 (2003).
[18]M. Zuin, R. Cavazzana, E. Martines, G. Serianni, *et al.*, Phys. Rev. Lett., **92**, 225003 (2004).
[19]W. F. Bergerson, C. B. Forest, G. Fiksel, D. A. Hannum, *et al.*, Phys. Rev. Lett., **96**, 015004 (2006).
[20]J. F. Hansen and P. M. Bellan, Astrophys. J., **563**, L183 (2001).
[21]H. Soltwisch, P. Kempkes, *et al.*, Plasma Phys. and Controlled Fusion, **52**, 124030 (2010).
[22]S. K. P. Tripathi and W. Gekelman, Phys. Rev. Lett., **105**, 075005 (2010).
[23]M. Yamada, H. Ji, S. Hsu, T. Carter, R. Kulsrud, N. Bretz, F. Jobes, Y. Ono, and F. Perkins, Phys. Plasmas, **4**, 1936 (1997).

The Princeton Plasma Physics Laboratory is operated
by Princeton University under contract
with the U.S. Department of Energy.

Information Services
Princeton Plasma Physics Laboratory
P.O. Box 451
Princeton, NJ 08543

Phone: 609-243-2245
Fax: 609-243-2751
e-mail: pppl_info@pppl.gov
Internet Address: http://www.pppl.gov